NeuroImage 231 (2021) 117837

Contents lists available at ScienceDirect

NeuroImage

journal homepage: www.elsevier.com/locate/neuroimage

The "when" and "where" of the interplay between attentional capture and response inhibition during a Go/NoGo variant

Joseph P. Happer[a], Laura C. Wagner[b], Lauren E. Beaton[b], Burke Q. Rosen[b,c,*], Ksenija Marinkovic[a,b,d]

[a] San Diego State University/University of California, San Diego Joint Doctoral Program in Clinical Psychology, 5500 Campanile Dr., San Diego 92182, CA, United States
[b] Department of Psychology, San Diego State University, 5500 Campanile Dr., San Diego 92182, CA, United States
[c] Department of Neurosciences, University of California, San Diego, 9500 Gilman Dr., La Jolla 92093, CA, United States
[d] Department of Radiology, University of California, San Diego, 9500 Gilman Dr., La Jolla 92093, CA, United States

ARTICLE INFO

Keywords:
Response inhibition
Attention
Cognitive control
Inferior frontal cortex
Medial prefrontal cortex
Magnetoencephalography

ABSTRACT

Inhibitory control relies on attention, inhibition, and other functions that are integrated across neural networks in an interactive manner. Functional MRI studies have provided excellent spatial mapping of the involved regions. However, finer temporal resolution is needed to capture the underlying neural dynamics and the pattern of their functional contributions. Here, we used anatomically-constrained magnetoencephalography (aMEG) which combines MEG with structural MRI to examine how the spatial ("where") and temporal ("when") processing stages and interregional co-oscillations unfold in real time to contribute to inhibitory control. Healthy participants completed a modified Go/NoGo paradigm in which a subset of stimuli was modified to be visually salient (SAL). Compared to the non-modified condition, the SAL manipulation facilitated response withholding on NoGo trials and hindered responding to Go stimuli, reflecting attentional capture effectuated by an orienting response to SAL stimuli. aMEG source estimates indicate SAL stimuli elicited the attentional "circuit breaker" effect through early activity within a right-lateralized network centered around the lateral temporal cortex with additional activity in the pre-supplementary motor area (preSMA) and anterior insula (aINS/FO). Activity of the bilateral inferior frontal cortex responded specifically to inhibitory demands and was generally unaffected by the attentional manipulation. In contrast, early aINS/FO activity was sensitive to stimulus salience while subsequent activity was specific to inhibitory control. Activity estimated to the medial prefrontal cortex including the dorsal anterior cingulate cortex and preSMA reflected an integrative role that was sensitive to both inhibitory and attentional stimulus properties. At the level of neurofunctional networks, neural synchrony in the theta band (4–7 Hz) revealed interactions between principal cortical regions subserving attentional and inhibitory processes. Together, these results underscore the dynamic, integrative processing stages underlying inhibitory control.

1. Introduction

A range of neurofunctional systems are needed to monitor one's behavior and adapt it to a dynamically changing environment. The ability to inhibit a response is an essential aspect of cognitive control. It relies on seamless integration across multiple neural networks subserving different functions such as attentional monitoring, working memory, motor planning, and response optimization. Functional imaging studies have provided excellent insight into the brain areas involved in these processes. However, the temporal resolution is inadequate to capture the underlying neural dynamics on a physiologically relevant time scale. To address this gap, the present study relies on a multimodal imaging approach to characterize spatiotemporal features and functional contributions of these parallel processes in real time as they unfold in an interactive manner. This level of understanding is needed for the realistic modeling of neural activity underlying inhibitory control with relevance for healthy behaviors and brain-based disorders (Breakspear, 2017).

Inhibitory control is frequently examined with the Go/NoGo and Stop Signal paradigms in which conflict arises between responding to the dominant "Go" stimuli and inhibiting a response to infrequent "NoGo" or "Stop" stimuli. Neuroimaging studies indicate that rapid response suppression activates a network of primarily prefrontal cortical (PFC; Aron et al., 2007; Swick et al., 2011), as well as subcortical regions such as the subthalamic nucleus of the basal ganglia (STN;

* Corresponding author at: 6505 Alvarado Rd. Suite 202, San Diego 92120, CA, United States.
E-mail addresses: jhapper@sdsu.edu (J.P. Happer), lwagner@sdsu.edu (L.C. Wagner), laurenbeaton11@gmail.com (L.E. Beaton), bqrosen@ucsd.edu (B.Q. Rosen), kmarinkovic@sdsu.edu (K. Marinkovic).

https://doi.org/10.1016/j.neuroimage.2021.117837
Received 26 July 2020; Received in revised form 25 January 2021; Accepted 3 February 2021
Available online 9 February 2021

Aron et al., 2007, 2014a; Duann et al., 2009; Nambu, 2004). These regions are recruited not only during outright stopping but also during response slowing (Wessel and Aron, 2013), suggesting a "braking" network (Aron et al., 2014a) that modulates implementation of inhibitory control. Even though numerous studies have focused on the right inferior frontal cortex (IFC) and its role in initiating response inhibition (Aron et al., 2014a; Duann et al., 2009; Rae et al., 2015), the functional contributions of other regions to overall braking performance are not well understood.

Presented unexpectedly, NoGo stimuli engage the attentional system which facilitates successful withholding of response (Wessel and Aron, 2013). Their low, "oddball" presentation frequency commonly activates a right-lateralized temporoparietal network including the temporoparietal junction (TPJ) and lateral temporal cortex (LTC), which may act as a "circuit breaker" to redirect attention to these salient stimuli (Boehler et al., 2011; Corbetta and Shulman, 2002; Downar et al., 2002). However, detection of infrequent stimuli also engages the ventrolateral and medial PFC areas (Braver et al., 2001; Halgren et al., 2011; Levy and Wagner, 2011; Manza et al., 2016), potentially conflating their contributions to inhibitory vs attentional control processes. In particular, the function of the right IFC within this attention/inhibitory dynamic has been a contentious issue (Aron et al., 2014b; Hampshire, 2015; Swick and Chatham, 2014). Some studies interpret this activation as being specific to response inhibition (Aron et al., 2014a) while others demonstrate right IFC activation during attentionally demanding tasks that do not require any behavioral inhibition (Correas et al., 2019; Halgren et al., 2011; Hampshire, 2015; Serences et al., 2005). Meta-analyses indicate functional parcellation of the right IFC with different areas subserving the two functions (Levy and Wagner, 2011). Previous studies have further attempted to address this issue by manipulating attentional demands within Stop Signal paradigms. However, findings have been mixed demonstrating both overlapping and distinct patterns of cortical activation between attentionally salient cues requiring a response and cues requiring outright stopping (Boehler et al., 2011; Chikazoe et al., 2008; Manza et al., 2016; Sharp et al., 2010).

Most of the relevant evidence comes from functional MRI (fMRI) studies which have provided precise spatial mapping of the cortical and subcortical regions involved in inhibitory and attentional processes. However, the temporal resolution of the underlying blood oxygen level-dependent (BOLD) signal is limited. The BOLD signal reflects local hemodynamic changes that are mediated by neurovascular coupling and unfold at a much slower pace than the underlying neural events (Buxton, 2002). As a result, the relative contributions of inhibitory and attentional networks may be obscured if measured in a temporally insensitive manner. Temporally precise methods, such as magnetoencephalography (MEG), have demonstrated their utility in delineating spatiotemporal stages of cognitive processing (Halgren et al., 2011; Kovacevic et al., 2012; Marinkovic, 2004). The neural oscillations recorded with MEG can be decomposed into spectral band ranges associated with neurofunctional processes (von Stein and Sarnthein, 2000). Oscillations in the theta range (4–7 Hz) are sensitive to cognitive effort (Kovacevic et al., 2012; Rosen et al., 2016; von Stein and Sarnthein, 2000), with co-oscillations (phase locking) in the theta range being particularly suitable for tracking integrative neural communication between cortical regions in real time (Beaton et al., 2018; Correas et al., 2019; Fries, 2005; Marinkovic et al., 2019).

In light of these considerations, the current study examined the interplay between inhibitory and attentional networks during a modified Go/NoGo paradigm in healthy adults. In this variant, participants responded to alternating "X" and "Y" letters (80%, Go) while trying to inhibit a response for each repetition (20%, NoGo). To evaluate the role of attention, 50% of NoGo stimuli were modified in size and color to be more visually salient (SAL) compared to non-modified (REG) NoGo stimuli, thus eliciting attentional capture. An equal number of Go stimuli were also modified to be salient. To examine the unfolding contributions of the relevant neurofunctional networks, we used an anatomically-constrained MEG (aMEG) approach that combines distributed MEG source modeling with structural MRI (Dale et al., 2000; Marinkovic, 2004). The aim of the study was twofold: to explore the "where" and "when" of the neural activation underlying inhibition and attentional processing in real time, and to elucidate the interactive processing reflected in neural synchrony between the principal cortical regions.

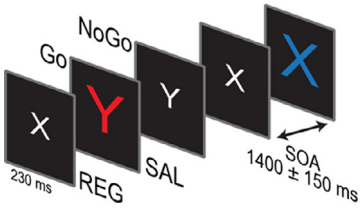

Fig. 1. *Go/NoGo task.* The task consisted of "X" and "Y" letters presented in an alternating (80%, Go) or repeated (20%, NoGo) manner. Participants were instructed to respond with their right hand to each alternation and inhibit their response to each repetition. To evaluate the role attention plays in inhibitory control, 50% of NoGo stimuli were modified in both size and color to be more visually salient (SAL) than the equiprobable non-modified (REG) NoGo stimuli. An equal number of Go stimuli were modified.

2. Materials and methods

2.1. Participants

Twenty-six (13 female; age = 28.8 ± 5.4 years (mean±SD)) right-handed, healthy volunteers participated in a MEG session and a structural MRI scan, in addition to filling out questionnaires. Participants reported no previous neurological, psychiatric or addiction-related problems, and none were on any medication at the time of the study. Given the inclusion of color within our stimulus parameters, all participants were screened for color blindness using the Ishihara Test (Ishihara, 1987). All participants gave written, informed consent and were compensated for their participation. Study procedures were approved by the Institutional Review Boards of the University of California, San Diego and San Diego State University.

2.2. Task

Participants performed a modified Go/NoGo task (Garavan et al., 2002) which consisted of "X" and "Y" letters presented in an alternating (80%, Go) or repeated (20%, NoGo) manner (Fig 1). Participants were instructed to make a right-hand response to each alternation as quickly and as accurately as possible and to inhibit their response to each repetition. Using Presentation (Neurobehavioral Systems), a total of 1440 trials were presented for 230 ms every 1400 ms ± a random incremental jitter of 150 ms. Stimuli subtended a horizontal visual angle of 0.97° and were presented in a white font on a black screen. To evaluate the role attention plays in response inhibition, 50% of NoGo stimuli (144 stimuli) were modified in both size and color to be more visually salient (SAL) than the equiprobable non-modified (REG) NoGo stimuli. An equal number of Go stimuli (144 stimuli) were modified to be salient as well. Thus, SAL stimuli comprised 20% of the total number of stimuli. To ensure salience, stimuli were presented in red, green, blue, or yellow colored font with a horizontal angle of 1.72°.

2.3. Data acquisition and analysis

2.3.1. MRI

Structural MRI images were acquired with a 1.5 T GE EXCITE HG whole-body scanner (General Electric) with a high-resolution T1-weighted IR-FSPGR scan (TR = 8.5 s, TE = 3.75 ms, TI = 500 ms, flip an-

gle = 10°, FOV = 240, 166 sagittal slices, 1.2 mm slice thickness, in-plane resolution 0.94 × 0.94 mm). Structural images were used to reconstruct each participant's cortical surface (Dale et al., 1999; Fischl et al., 1999) which served to constrain inverse source estimates. The inner skull surface was used as a boundary element model of volume conductor in the forward calculations. For the purposes of intersubject averaging, the reconstructed surface was morphed onto an average brain representation (Fischl et al., 1999). The solution space was approximated by ~5000 free-rotating dipoles spaced ~7 mm apart.

2.3.2. MEG

MEG signals were recorded from 204 channels comprising 102 pairs of planar gradiometers using a whole-head Vectorview system (Elekta Neuromag) in a magnetically and electrically shielded room. The signals were continuously recorded with 1000 Hz sampling rate and minimal filtering (0.1 to 330 Hz). Four head position indicator coils attached to the head, main fiduciary points including the nasion and preauricular points, and a large array of random points across the scalp were digitized with 3Space Isotrak (Polhemus Inc.) to allow for subsequent precise co-registration with structural MRI images. Only trials with correct responses were included in the analysis. To mitigate possible statistical bias, the number of trials was equated across the four trial conditions (REG Go, REG NoGo, SAL Go, SAL NoGo) for each subject by randomly sampling trials for each condition until a number equal to the condition with the fewest trials was attained. This resulted in an average of 97 (±14) trials per condition per person.

2.3.2.1. Event-related fields (ERFs); source estimates in time domain. MEG data analysis was performed using custom Matlab functions which rely in part on publicly available packages including FieldTrip (Oostenveld et al., 2011), EEGLAB (Delorme and Makeig, 2004), and MNE (Gramfort et al., 2014). Continuous data were first bandpass filtered from 0.1 to 30 Hz. Epochs extending −300 ms to 800 ms relative to the stimulus onset were baseline corrected using the prestimulus period as the baseline. Each epoch was downsampled to 250 Hz and visually inspected for movement artifacts. Additional artifacts such as heartbeat and eye blinks were removed using independent component analysis (Delorme and Makeig, 2004). Noise-normalized source estimates were calculated with the linear minimum-norm estimation procedure and were constrained to the cortical surface (Dale et al., 2000; Dale and Sereno, 1993; Hamalainen and Ilmoniemi, 1994). Noise covariance was calculated from the prestimulus periods across data epochs and used for inverse calculation resulting in "brain movies" or dynamic statistical parametric maps (dSPM) that are inspired by the statistical maps used to analyze fMRI data but with excellent temporal resolution. The noise-normalized estimates of the cortical current dipole power ameliorate the point-spread function and result in a good spatial uniformity across the surface (Dale et al., 2000; Liu et al., 2002). The source estimates reflect the likelihood that a particular patch of cortex is more active than baseline at each time point and are expressed as the square root of an *F* statistic (Dale et al., 2000; Marinkovic et al., 2014).

2.3.2.2. Region-of-interest analysis. Region-of-interest (ROI) analysis was conducted to further investigate the possible effects of attentional capture and response inhibition on ERFs. Unbiased ROIs were based on the overall grand average source power estimates across all participants and conditions and comprised the cortical dipole locations with most notable cortical activity. Furthermore, the same set of ROIs was used for all participants in a manner blind to their individual activations by means of an automatic morphing procedure (Fischl et al., 1999). Specifically, bilateral ROIs encompassed areas in the medial prefrontal cortex including the dorsal anterior cingulate cortex (ACC) and pre-supplementary motor area (preSMA), the inferior frontal cortex (IFC), the lateral temporal cortex (LTC), temporoparietal junction (TPJ), right parietal area (PAR), right anterior insula/frontal operculum (aINS/FO), right lateral occipital area (OCC), and the left sensorimotor hand region (sMOT). Estimated time courses for each condition were extracted for each subject and averaged into grand mean waveforms.

2.3.2.3. Co-oscillations: phase locking in theta band (4–7 Hz). Phase locking values (PLV) reflect long-range co-oscillations between cortical regions by measuring inter-trial consistency of the phase angle between two ROIs (Lachaux et al., 1999). First, continuous data were bandpass filtered from 0.1 to 100 Hz then segmented into epochs extending −300 to 800 ms relative to stimulus onset plus an additional 300 ms of padding on each end resulting in a total epoch length of −600 to 1100 ms. The same ERF artifact rejection process was used to remove movement, eye blinks, and heartbeat. A complex power spectrum was calculated across all trial epochs with Morlet wavelets in 1 Hz increments in the theta frequency band (4 to 7 Hz), with wavelet width varying from 2 to 3.5 cycles to ensure a constant frequency resolution of 2 Hz and time resolution of 80 ms. To prevent edge artifacts, the padding was discarded after the wavelet analysis. Source estimates were calculated using the anatomically-constrained method described above for ERFs. However, to prevent biasing the inverse solution against spontaneous brain oscillations, the noise covariance used for inverse calculation was estimated from the empty room data pooled across recording sessions and bandpass filtered between 3 and 50 Hz. A signal-to-noise ratio (SNR) of 5 (Lin et al., 2004) was used for scaling of the noise covariance in calculation of the inverse operator. An identity matrix was used for the noise-sensitivity normalization of the source-space solution. The noise-sensitivity normalized estimates of total source power were obtained for each frequency at each location on the cortical surface. At each frequency step within the theta band, PLVs were computed for pairs of ROIs identified through ERF analysis, averaged across frequency bands, and expressed as percent change relative to baseline (Beaton et al., 2018; Correas et al., 2019; Marinkovic et al., 2019).

2.3.3. Statistical analyses

Statistical analyses for all data proceeded using similar methodology using Repeated Measures ANOVAs where trial type (Go, NoGo) and stimulus salience (REG, SAL) served as within-subject factors, where appropriate. For ERFs and PLVs, data were averaged over the time windows of interest prior to being entered into the ANOVAs. Time windows were chosen to capture prominent peaks in the grand-average time courses of noise-normalized estimates of cortical current dipole power across all participants and conditions. Roughly equivalent time windows were chosen that encapsulated peak PLV increases. These time windows reflect successive processing stages: attentional capture, interplay between attentional capture and response inhibition, and response inhibition and execution. *F*-values for the main effects of trial type and stimulus salience for ERF and PLV time windows are presented in Table 1 while Trial Type x Stimulus Salience interactions and pairwise comparisons are presented in text unless otherwise noted.

2.3.4. Materials and data availability

Data files used in the main analyses presented here have been archived and uploaded to FigShare and are freely available at 10.6084/m9.figshare.c.5239850.v1.

3. Results

3.1. Performance

Salient stimuli were successful at capturing attention which was reflected in longer reaction times (RTs) to SAL ($M \pm SD = 455 \pm 100$ ms) compared to REG stimuli (406 ± 87 ms), $F(1,25) = 82.2$, $p < 0.001$ (Fig 2). The SAL condition may have acted as a "circuit breaker" as orienting to novelty facilitated response withholding. This was reflected in an attentional effect on response accuracy yielding a Trial Type x

Table 1

Summary of ANOVAs of event-related fields and theta PLV for different ROIs. Included are the main effects of stimulus salience (SAL, REG) and trial type (NoGo, Go). Time windows were selected and displayed based on the activity of measurable peaks. aINS/FO: anterior insula/frontal operculum; ACC: dorsal anterior cingulate cortex; IFC: inferior frontal cortex; LTC: lateral temporal cortex; PAR: parietal area; preSMA: pre-supplementary motor area; TPJ: temporoparietal junction; sMOT: sensorimotor cortex. Significance level is indicated as follows: $^{\dagger}p < 0.10$; $^{*}p < 0.05$; $^{**}p < 0.01$; $^{***}p < 0.001$; $^{****}p < 0.0001$. For the sMOT-lh activation and sMOT-lh—preSMA-lh PLV, Response inhibition represents Go > NoGo.

	Attention capture (SAL > REG) $F(1,25)$	Response inhibition (NoGo > Go) $F(1,25)$	Attention capture (SAL > REG) $F(1,25)$	Response inhibition (NoGo > Go) $F(1,25)$	Attention capture (SAL > REG) $F(1,25)$	Response inhibition (NoGo > Go) $F(1,25)$
Event-related fields	**140–180 ms**		**200–375 ms**		**400–450 ms**	
LTC-lh	15.7***	0.7	12.2**	24.1***	2.6	23.4****
LTC-rh	27.8****	0.0	16.8***	6.3*	6.4*	12.5*
TPJ-rh	30.8****	0.3	23.6****	7.9**	13.9***	11.8**
PAR-rh	13.0**	0.0	20.8***	6.0*	2.8	6.0*
preSMA-lh	10.1**	1.0	3.6†	14.7***	2.0	9.9**
preSMA-rh	5.0*	0.0	6.7*	9.7**	2.4	13.2**
ACC-rh	5.9*	5.5*	5.4*	28.0****	0.2	8.0**
aINS/FO-rh	13.8**	0.8	3.1†	23.7****	0.0	4.1†
IFC-lh	2.0	2.2	1.0	16.9***	0.6	1.5
IFC-rh	0.3	1.6	1.6	21.8****	2.7	10.2**
sMOT-lh	0.4	1.5	0.0	1.5	0.9	7.9**
Theta PLV	**125–225 ms**		**200–350 ms**		**400–450 ms**	
IFC-rh—sMOT-lh	4.5*	0.4	0.0	2.0	0.2	0.4
LTC-rh—PAR-rh	6.8*	0.2	5.6*	0.9	0.6	2.5
LTC-rh—preSMA-lh	9.8**	0.6	2.6	1.8	0.2	0.1
IFC-lh—preSMA-lh	0.1	2.0	0.0	10.4**	0.3	2.8
IFC-rh—IFC-lh	0.2	6.4*	0.2	12.9**	1.1	6.8*
IFC-rh—PAR-rh	7.1*	5.6*	9.8**	18.8***	1.3	10.8**
IFC-rh—preSMA-lh	0.7	1.3	0.0	7.2*	0.3	1.3
sMOT-lh—preSMA-lh	0.0	0.1	1.6	3.4†	1.4	18.3***

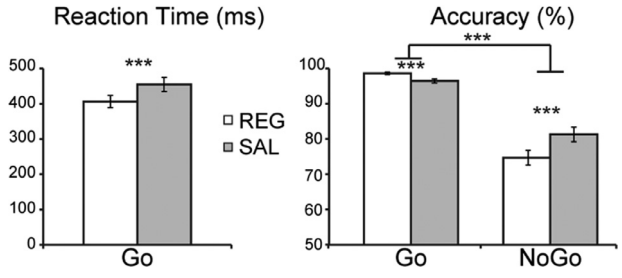

Fig. 2. *Task Performance.* Participants had slower reaction times (RTs) on salient (SAL) compared to regular (REG) Go stimuli. Furthermore, relative to the REG condition, the accuracy was lower on SAL Go trials and higher on SAL NoGo trials, consistent with the SAL-induced attentional capture acting as a "circuit breaker." As expected, response accuracy was overall higher on Go trials compared to NoGo trials. Error bars represent ±SEM. $^{***} = p < 0.001$.

Salience interaction, $F(1,25) = 48.5$, $p < 0.001$, as SAL stimuli improved response inhibition on NoGo trials, $F(1,25) = 35.2$, $p < 0.001$, while the same effect hindered response execution on SAL Go trials, $F(1,25) = 42.6$, $p < 0.001$. As expected, response accuracy was higher on Go compared to NoGo trials overall, $F(1,25) = 86.2$, $p < 0.001$.

3.2. Spatiotemporal aMEG estimates

The spatiotemporal processing stages elicited by the Go/NoGo task revealed both distinctive and overlapping networks underlying attentional capture and response inhibition (Fig 3, for an expanded figure see Supplementary Figure 1). Attentional capture was reflected in an early right-lateralized increase of neural activity along the ventral visual network. This was followed by activation of a bilateral network of cortical regions sensitive to response inhibition, particularly in the IFC bilaterally. The dorsal anterior cingulate cortex (ACC) and pre-supplementary motor area (preSMA) in the medial PFC served as intermediary areas, showing sensitivity to both attentional and inhibitory dimensions. Neural activity of the sensorimotor hand area (sMOT) reflected motor preparation and execution.

3.2.1. Early activity to attentional capture (140–180 ms)

Fig. 3 illustrates a time line of neural activity of the cortical regions in which SAL stimuli elicited overall greater activation than REG stimuli (Table 1). The earliest main effects of stimulus salience were noted to peak at ~120 ms within the OCC, $F(1,25) = 17.3$, $p = 0.0003$, and PAR, $F(1,25) = 9.0$, $p = 0.006$. Subsequent activity was particularly evident over the right-dominant posterior cortex including the right TPJ and LTC. While the SAL-REG difference was observed bilaterally in the LTC, the SAL-induced activity of the right LTC was much stronger overall compared to the left LTC, $F(1,25) = 23.4$, $p < 0.0001$. In addition, sensitivity to visual salience at this latency was also observed in the medial frontal cortex, including the bilateral preSMA and right ACC, and the right aINS/FO.

3.2.2. Interplay between attentional capture and response inhibition (200–375 ms)

Elevated SAL-induced activity was maintained within this attention-sensitive network. The right TPJ and right parietal area (PAR) also sustained greater activity in response to SAL stimuli at this stage (Table 1). Furthermore, NoGo trials elicited greater activity compared to Go trials in the right LTC, TPJ, and PAR, highlighting involvement of the attentional component in inhibitory control.

In contrast, bilateral IFC regions responded preferentially to the inhibitory demands of NoGo trials and were not affected by the attentional features of SAL stimuli. However, the right frontal cortex did exhibit some sensitivity to the SAL manipulation. The right aINS/FO demonstrated a trend for SAL stimuli to elicit an overall increase in activity compared to REG. Likewise, within the right IFC, SAL-induced activity was specific to Go trials compared to the REG counterpart, $F(1,25) = 4.7$, $p = 0.04$. In contrast, NoGos were unaffected by stimulus salience, $F(1,25) = 0.0$, $p = n.s.$ Overall, the activity in the left and right IFC did not differ at this time. The mPFC demonstrated sensitivity to both inhibition and attentional demands. More specifically, the

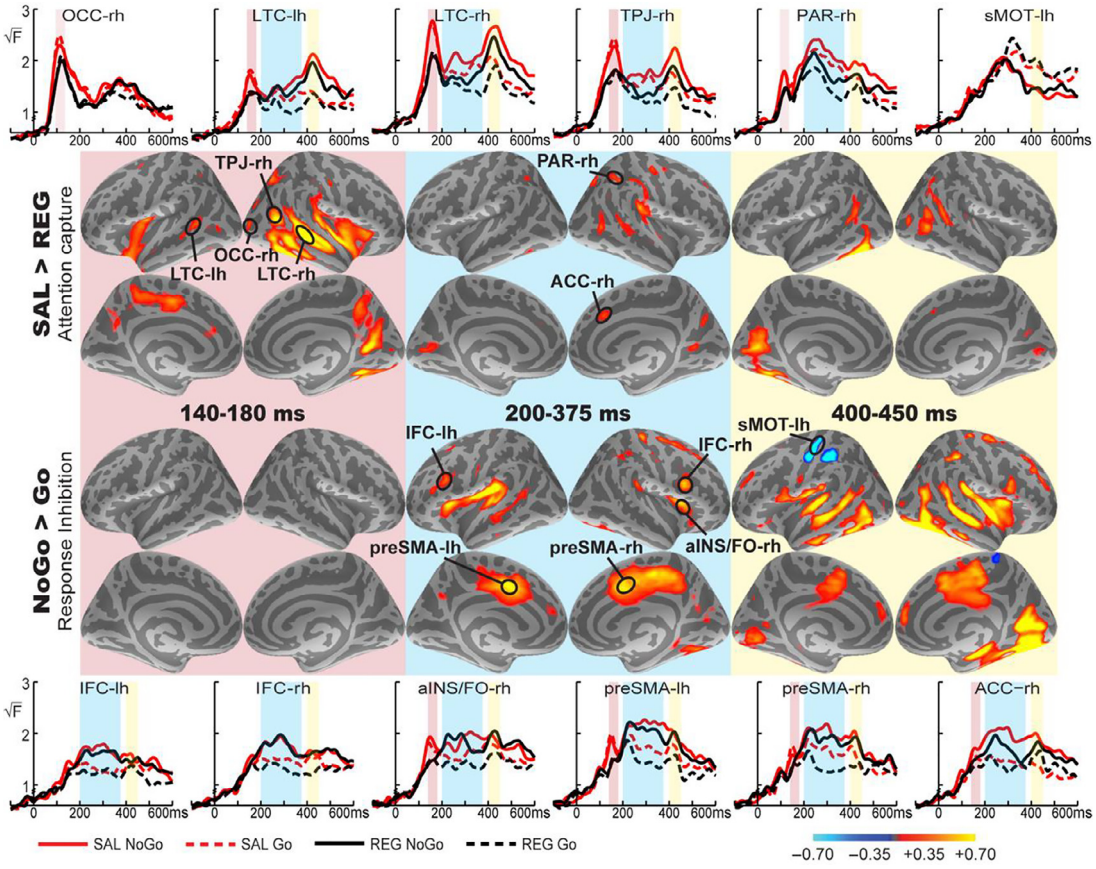

Fig. 3. *Group average maps and timecourses of estimated dipole strengths.* The effects of attention-evoking visual salience are presented as subtraction maps representing the overall main effect of stimulus salience (SAL > REG), and the timecourses showing how the activity unfolds across time starting with an early peak in the occipital cortex (OCC-rh). Right-dominant areas including the lateral temporal cortex (LTC), the temporoparietal junction (TPJ), the parietal area (PAR), and anterior insula/frontal operculum (aINS/FO) as well as the pre-supplementary motor area (preSMA) medially are particularly sensitive to attentional capture. SAL stimuli induced peak activation of the attention network shortly after stimulus onset (red shading), but activity was maintained for the duration of the trial. A network subserving response inhibition was likewise identified using subtraction maps of the main effect of trial condition (NoGo > Go) and included bilateral inferior frontal cortex (IFC), aINS/FO, and subregions of the medial prefrontal cortex: the anterior cingulate cortex (ACC), and preSMA. However, both the ACC and preSMA acted as intermediary regions, sensitive to both attentional capture and response inhibition (blue shading). Engagement of the primary somatosensory motor area (sMOT-lh) was observed just prior to responding (yellow shading). For an expanded version of this figure that includes contrasts for simple main effects, see Supplementary Figure 1.

ACC was differentially affected as indicated by a Trial Type x Salience interaction, $F(1,25) = 4.5$, $p = 0.043$, such that SAL NoGos elicited the greatest activity compared to all other stimuli (p's < 0.01) while REG NoGos evoked greater activation than Go stimuli (p's < 0.01), which did not differ from each other. Similarly, the preSMA showed strong bilateral activity to inhibitory demands while maintaining overall greater sensitivity to SAL stimuli. Indeed, the right preSMA exhibited a strong trend for a Trial Type x Salience interaction, $F(1,25) = 4.0$, $p = 0.056$, which indicated that SAL Gos elicited greater activity than the REG Gos, $F(1,25) = 11.9$, $p = 0.002$. In contrast, stimulus salience did not impact NoGo activity, $F(1,25) = 1.2$, $p = n.s.$ The potential impact of this dual sensitivity is suggested by a positive correlation between the overall SAL-REG activity difference of the left preSMA and SAL NoGo accuracy ($r = 0.46$, $p = 0.018$) and SAL Go RTs ($r = 0.40$, $p = 0.042$).

3.2.3. Response inhibition and execution (400–450 ms)

The posterior temporoparietal areas continued to exhibit increased activity in response to both attentional capture and inhibition (see Table 1), suggesting their involvement not only in the early detection of visually salient stimuli but also to NoGo-evoked inhibition. At this time, activity in the bilateral preSMA, right ACC, and right IFC was specific to response inhibition, which may reflect their involvement in conflict resolution between response facilitation and inhibition (Braver et al., 2001; Kovacevic et al., 2012; Nachev et al., 2008; Ridderinkhof et al., 2004). However, the right IFC, continued to exhibit increased SAL-induced activity for Go trials relative to REG, $F(1,25) = 8.4$, p=0.008. Go trials elicited greater activation in the sMOT-lh starting at ~300 ms in preparation for making a response.

3.3. Theta co-oscillations

Analysis of phase locking values (PLVs) in the theta band range revealed widespread co-oscillations between multiple cortical regions (Fig 4, Table 1). Attentional capture from SAL stimuli elicited an increase in phase synchrony that peaked at ~175 ms. During this time, the right LTC appeared to function as an attentional "hub" in response to SAL stimuli, as it demonstrated coordinated synchrony with both the preSMA and PAR with relevance to attention. SAL-induced attentional capture also elicited an increase in PLV between the right IFC and left sMOT at this latency.

A network of regions responded specifically to the inhibitory demands of NoGo trials, peaking at ~300 ms. This was evidenced by increased PLVs between the preSMA and bilateral IFC, as well as co-oscillations between the right and left IFC. At this time, phase locking between the right IFC and PAR demonstrated dual engagement by both inhibition and attentional demands. Increased co-oscillations of the right IFC with areas across the two networks supports its essential role in binding these domains into an integrated representation in service of successful inhibition.

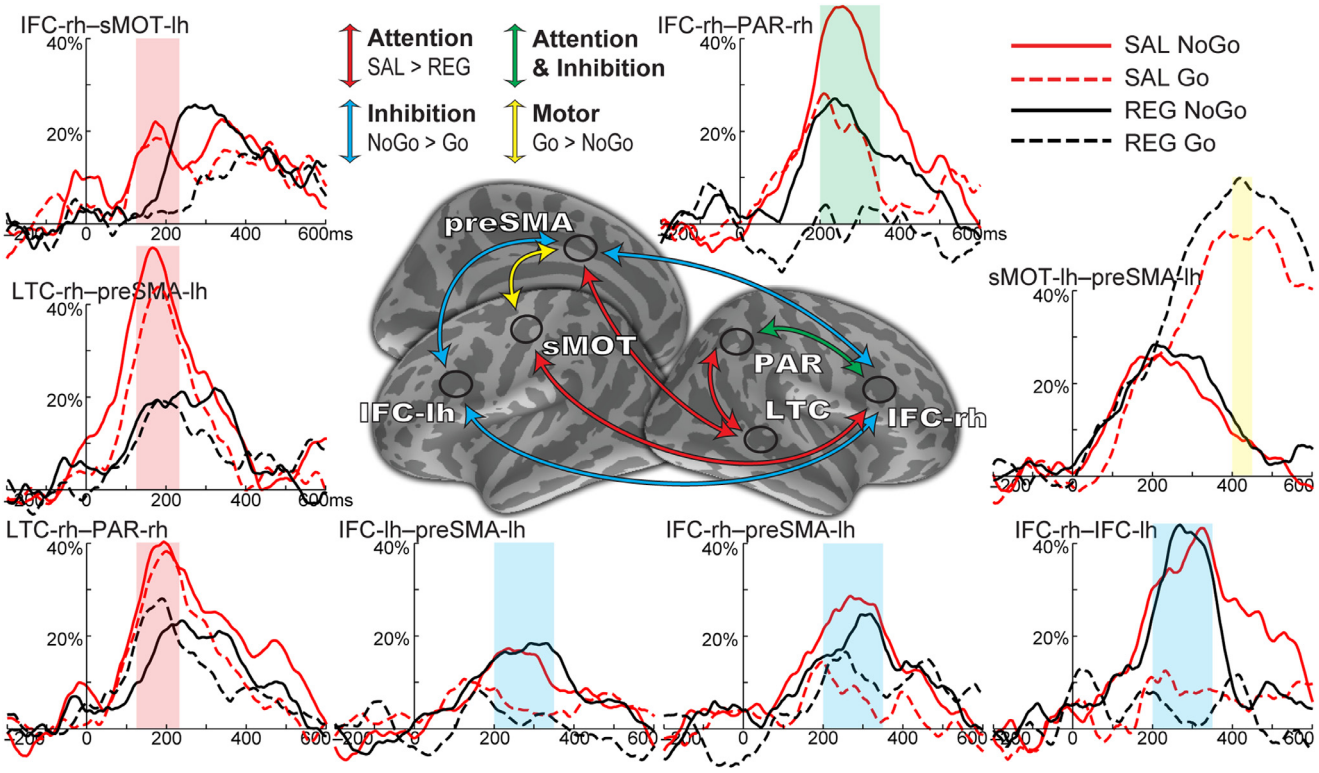

Fig. 4. *Group average phase locking values (PLVs) between cortical regions in the theta band, expressed as percent change from baseline.* Attentional processing centered around the right lateral temporal cortex (LTC), which acted as a "hub" given its increased PLVs with regions involved in both attention (parietal area: PAR) and inhibition (pre-supplementary motor area: preSMA). Salient stimuli (SAL) also induced early phase synchrony between the right inferior frontal cortex (IFC) and the left sensorimotor hand area (sMOT), suggestive of rapid suppression of motor output. The bilateral IFC and preSMA co-oscillations responded specifically to the inhibitory demands of NoGo stimuli, creating a "braking" network. Additionally, synchrony between the right IFC and PAR increased along both attention and inhibitory stimulus properties. Finally, the sMOT—preSMA connection reflected engagement of the motor system to Go stimuli and was unaffected by bottom-up visual salience.

Within the motor network, all stimuli elicited an initial increase in PLV between the left sMOT and preSMA during a nonspecific motor preparation stage. However, phase locking subsided for NoGos but continued to increase for Gos until approximately the time of response execution (~400 ms).

4. Discussion

This study utilized a temporally-sensitive aMEG approach to examine the interplay between attentional and inhibitory demands imposed by a modified Go/NoGo paradigm. The results revealed both distinctive and overlapping spatiotemporal characteristics of the networks underlying these two processing streams. The principal findings can be summarized as follows: (1) attentional capture resulted in a momentary response "brake" that (2) elicited early activation of right-lateralized temporo-parietal cortical areas; (3) subsequent neural activity of the bilateral IFC responded specifically to inhibitory demands while (4) the mPFC was uniquely sensitive to an interplay between attentional capture and response inhibition; (5) activity within the primary sMOT was specific to response execution and unaffected by the attentional manipulation; (6) finally, theta phase synchrony revealed long-range co-oscillations between the principally involved cortical regions providing an insight into how attentional, inhibitory, and integrative aspects unfold at a network level in real time.

4.1. Attentional capture

SAL stimuli captured attention which was reflected in *improved* response inhibition on NoGo trials but *impaired* response execution on Go trials. As expected, both of these effects resulted from momentary response braking, supporting the premise that infrequent, unexpected stimuli act as an attentional "circuit breaker" to disrupt ongoing processes (Frank, 2006; Horstmann, 2006; Wessel, 2018; Wessel and Aron, 2017). This has been described as an orienting response (Halgren and Marinkovic, 1995; Sokolov, 1963) which is accompanied by phasic arousal (Marinkovic et al., 2001) and suspension of motor activity (Wessel, 2018; Wessel and Aron, 2013, 2017). Recent evidence and theories suggest that this "circuit breaker" effect may in fact be effectuated by activation of a "hyperdirect" pathway via the subthalamic nucleus (STN) of the basal ganglia shortly after the appearance of unexpected stimuli (Frank, 2006; Haynes and Haber, 2013; Wessel, 2018; Wessel and Aron, 2017). Indeed, motor slowing following salient stimuli was absent in mice whose STN had been deactivated (Heston et al., 2020), supporting the involvement of the STN in motor suppression. As the brain is engaged in continuous task-relevant processing, the momentary SAL-induced disruption must be overcome in order to execute a response (Chikazoe et al., 2008; Frank, 2006; Horstmann, 2006). In the present study, SAL Go stimuli interrupted an otherwise prepotent tendency to respond, requiring re-initiation of the motor action and resulting in longer reaction times compared to REG Go trials. At the same time, SAL-evoked braking was favorable on NoGo trials as it facilitated response inhibition. Alternatively, the observed results could be explained by an "expectation" effect of the SAL stimuli, which due to the task design, appear with higher probability on NoGo than on Go trials. Thus, participants could expect that a SAL trial is a NoGo trial, which would engage inhibitory control processes. The increased likelihood of withholding their response would result in increased accuracy on NoGo and decreased accuracy and longer RTs on Go trials for SAL stimuli.

As shown in Fig 3, SAL stimuli induced neural activity at ~160 ms in a highly right-lateralized network of cortical regions. It was estimated primarily to the right LTC and TPJ which encompassed the posterior aspects of the superior temporal sulcus. It has been established that activation of the right ventral attention system is driven by stimulus properties in a bottom-up fashion, with novel or salient stimuli capturing attention (Corbetta and Shulman, 2002) consistent with the right-dominant activity elicited by SAL stimuli (Langner et al., 2012). The TPJ in particular is an essential region for reorienting attention to oddball stimuli across multiple sensory modalities (Corbetta and Shulman, 2002; Downar et al., 2002). Similarly, the right LTC is activated by detection of infrequent, salient stimuli (Corbetta and Shulman, 2002; Halgren et al., 1995, 2011). Importantly, the SAL-induced activity of the right TPJ and LTC observed in the present study is consistent with the timing and pattern of activity elicited by oddball stimuli in a previous aMEG study (Halgren et al., 2011) and confirmed with direct intracranial recordings during oddball (Halgren et al., 1995) and spatial attention paradigms (Martin et al., 2019). Expanding on these findings, the theta band synchrony observed during the early, attentional stage underscores the importance of the right LTC, which may have acted as a "hub" for attentional processing and integration with other cortical regions such as the parietal area and preSMA. The central role of the LTC within an interactive cortical network subserving a variety of cognitive processes (Hein and Knight, 2008) is supported by its widespread cortical projections (Morecraft et al., 1993). Overall, these findings indicate that a right-lateralized ventral attention network is activated by the unexpected SAL features. These bottom-up attentional effects could then affect ongoing cognitive and motor processes (Wessel and Aron, 2017) through interactions with other regions.

Outside of the temporo-parietal cortex, the medial PFC, particularly the preSMA, and the aINS/FO were the only regions that showed selective early activity to SAL stimuli. Activity peaked at ~160 ms which is consistent with aMEG activity to oddball tones (Halgren et al., 2011) and intracranial EEG recordings during successful motor inhibition on stop trials (Swann et al., 2009, 2012). Furthermore, this timing aligns with reports of global suppression of motor excitability at ~150 ms elicited by the appearance of unexpected stimuli (Wessel and Aron, 2013, 2017). It has been suggested that the aINS/FO in particular is sensitive to salient events and is a major hub in the salience network (Uddin, 2015) subserving both attentional orienting and subsequent cognitive processing (Menon and Uddin, 2010; Sridharan et al., 2008). Additionally, the aINS/FO as part of the right PFC more broadly and the preSMA are part of a network that effectuates rapid suppression of motor output via the "hyperdirect" pathway which includes the STN of the basal ganglia (Aron et al., 2014a; Frank, 2006; Nambu, 2004). It is engaged by unexpected stimuli (Heston et al., 2020; Wessel and Aron, 2013, 2017) with powerful inhibitory downstream effects on the primary motor cortex (Stinear et al., 2009; Swann et al., 2009). In the present study, possible engagement of the hyperdirect pathway by SAL stimuli is suggested by theta phase locking between the right IFC and left sMOT shortly after stimulus onset (~175 ms) specifically in response to SAL stimuli, which is consistent with a "circuit breaker" effect (Corbetta and Shulman, 2002; Wessel and Aron, 2017).

Subsequent activity of the attentional stream including the right LTC, TPJ, and PAR began to increase in response to NoGo stimuli starting after ~200 ms and continued until shortly before response execution (~425 ms). This shift from bottom-up, stimulus-driven processing to task-related activity elicited primarily by NoGo stimuli is consistent with intracranial generators of ERPs to infrequent, behaviorally relevant events (Halgren et al., 1995) and fMRI-based patterns of activation during attentional capture and control (Boehler et al., 2011; Serences et al., 2005).

4.2. Response inhibition

One aim of the present study was to shed light on the contentious interpretation of the function of the right IFC. Some accounts attribute it to the attentional engagement by infrequent stimuli (Hampshire, 2015) and others emphasize its central involvement in response inhibition (Aron et al., 2014a). Most of the research has been conducted using the fMRI BOLD signal whose temporal resolution is unable to resolve the relative timing of these contributions. The multimodal aMEG approach applied here is sensitive to the processing sequence and can provide insight into the underlying spatiotemporal stages. The results of the present study are consistent with the accounts favoring response inhibition (Aron et al., 2014a) and confirm that, indeed, the right IFC responds selectively to the NoGo inhibitory demands. Importantly, the right IFC is insensitive to the attentional dimension as the SAL manipulation had no effect on NoGo-induced activation. Furthermore, the latency of this effect aligns with timing reported in studies using intracranial EEG recordings during stop signal paradigms (Swann et al., 2009, 2012). In contrast, while the right aINS/FO initially responded to stimulus salience, subsequent activation was more specific to the inhibitory control demands of NoGo stimuli regardless of the attentional manipulation, supporting its involvement in cognitive control (Aron et al., 2014a; Menon and Uddin, 2010; Sridharan et al., 2008; Swick et al., 2011). This dual sensitivity across time underscores the need for temporally precise methods that can elucidate neural activity related to processing stages, which might otherwise have been conflated or obscured using BOLD-related methods. Overall, these results support previous fMRI studies that have demonstrated preferential activation of the right IFC to inhibitory demands even after controlling for attentional manipulations (Boehler et al., 2011; Chikazoe et al., 2008; Sebastian et al., 2016).

However, while prevailing theories suggest a right-lateralized braking network centered around the right IFC (Aron et al., 2014a), our aMEG estimates revealed bilateral IFC involvement. These results are consistent with previous neuroimaging studies (Manza et al., 2016; Sebastian et al., 2016; Sharp et al., 2010; Swick et al., 2011), suggesting inhibitory control may be subserved by a bilateral network rather than a singular node (Swick et al., 2011). An inhibitory control network is further supported by previous MRI-based measures of functional connectivity which indicate increased co-activation of the right IFC with both the left IFC and preSMA during inhibitory control paradigms (Duann et al., 2009; Rae et al., 2015; Sebastian et al., 2016). The present study confirms and expands on these findings using interregional phase locking analyses between the right and left IFC and between these regions and the preSMA. Co-oscillations among these regions preferentially increased for NoGo trials but were unaffected by the SAL manipulation, suggesting a network that responds specifically to inhibitory demands. Moreover, widespread cortical projections from these regions provide additional support for the formation of braking network (Aron et al., 2007; Medalla and Barbas, 2009). Phase synchrony between the right IFC and PAR was uniquely affected by both attentional and inhibitory stimulus properties. Thus, the right IFC may provide an integrative link helping to modulate activation of the braking network (Duann et al., 2009; Rae et al., 2015).

4.3. Integrative processing

In the present study, activity within the mPFC peaked at ~275 ms and exhibited complex involvement in the detection and processing of behaviorally salient events while also contributing to motor inhibition. Extensive neuroimaging evidence indicates the mPFC is essential for top-down regulation and implementation of cognitive control, particularly to override prepotent, automatic responses (Braver et al., 2001; Kovacevic et al., 2012; Nachev et al., 2008; Ridderinkhof et al., 2004; Rosen et al., 2016). This was confirmed in the current study where the inhibitory demands of the NoGo trials evoked overall greater mPFC ac-

tivity compared to Go trials. However, the SAL manipulation had differential effects on mPFC regions. Within the ACC, SAL-induced activity was specific to NoGo trials, reflecting the contributions of the ACC to the detection and resolution of conflicting response options (Braver et al., 2001; Kovacevic et al., 2012; Manza et al., 2016; Ridderinkhof et al., 2004; Rosen et al., 2016). In contrast, within the preSMA, the SAL manipulation selectively increased Go activity which correlated with longer RTs. This finding is consistent with extensive literature indicating that the preSMA is recruited during suppression and slowing of motor responses (Aron et al., 2007, 2014a; Duann et al., 2009; Nachev et al., 2008; Rosen et al., 2016; Sharp et al., 2010; Swann et al., 2012; Swick et al., 2011). Furthermore, phase locking analyses revealed widespread communication centered around the mPFC and between regions associated with attention, inhibition, and motor execution. This highlights the integrative nature of the mPFC which is supported by its widespread anatomical and functional connections with other regions (Aron et al., 2007; Beaton et al., 2018; Duann et al., 2009; Marinkovic et al., 2019; Medalla and Barbas, 2009; Morecraft et al., 1993; Nachev et al., 2008; Nambu, 2004; Rae et al., 2015). Overall, these findings underscore how the mPFC is uniquely situated to be an integrative "hub" given the convergence of both top-down and bottom-up stimulus processes combined with connections to motor output.

4.4. Response execution

Even though the lateral and medial PFC contribute to response selection and planning (Nachev et al., 2008; Ridderinkhof et al., 2004), execution or inhibition of a response is ultimately enacted at the primary sMOT (Nachev et al., 2008; Stinear et al., 2009). Through this process, corticospinal tracts are either excited for response facilitation or inhibited for response suppression in a generalized manner (Stinear et al., 2009). In light of these considerations, bottom-up stimulus properties should not influence activation of the sMOT, which is indeed supported by the results of the present study where the SAL manipulation had no effect on sMOT activity and is consistent with previous reports (Kovacevic et al., 2012). Phase locking analyses between the preSMA and sMOT expand on this to further suggest that communication between the medial and lateral motor areas is based specifically on motor facilitation or suppression. These data together indicate that the motor system is overall unaffected by sensory stimulus properties.

4.5. Conclusion

In sum, this study examined the contributions of attentional capture and response inhibition to inhibitory control during a Go/NoGo task modified to probe both functions. A multimodal approach provided insight into spatiotemporal characteristics of both processing dimensions as they unfolded in real time. The SAL manipulation resulted in a momentary "brake" during response preparation which facilitated response withholding to NoGo trials and impeded responding to Go stimuli. During an early processing stage, the visual salience elicited increased activity of right-dominant posterior cortical areas particularly in the LTC and TPJ, but also in the preSMA and aINS/FO. Subsequent bilateral activity of the IFC was specific to the inhibitory demands of NoGo trials and generally unaffected by the SAL manipulation. Our findings are consistent with extensive evidence suggesting the selective tuning of the IFC for inhibition, although we did not observe the right IFC dominance which has been reported. However, the right aINS/FO exhibited dual sensitivity with early activity elicited by SAL stimuli, highlighting its role as a hub within a salience detection network (Menon and Uddin, 2010; Sridharan et al., 2008; Uddin, 2015), while later activity was specific to inhibitory control demands. The mPFC, including the ACC and the preSMA, was sensitive to both attentional and inhibition stimulus properties, supporting its integrative, top-down role during response conflict and selection (Braver et al., 2001; Kovacevic et al., 2012; Nachev et al., 2008; Ridderinkhof et al., 2004). Finally, responses were executed by the primary sMOT, which was unaffected by bottom-up salience. Theta co-oscillations between principally involved cortical regions support the formation of integrative and interactive networks subserving the attentional and inhibitory processes of response inhibition (Correas et al., 2019; Marinkovic et al., 2019). While these findings were observed in a young, healthy population, evidence indicates the spatiotemporal dynamics of inhibitory control may change with age (Knezevic and Marinkovic, 2017; Lin et al., 2018). This in conjunction with our current results highlight the need for further investigations across the lifespan using temporally sensitive methods which have implications for the realistic modeling of neural dynamics underlying healthy behaviors and brain-based disorders.

Author statements

Conceptualization, K.M.; Methodology, K.M. and B.Q.R.; Investigation, B.Q.R., L.C.W., L.E.B., J.P.H.; Formal Analysis, J.P.H.; Writing – Original Draft, J.P.H and K.M.; Writing – Review & Editing, J.P.H. and K.M.; Software, B.Q.R., L.E.B., L.C.W., J.P.H.

Declaration of Competing Interest

The authors declare no competing interests.

Acknowledgments

This research was supported by funds from the National Institutes of Health (R01-AA0166224, T32-AA013525, & F31-AA028437). The authors would like to thank the member of the SpatioTemporal Brain Imaging Lab, particularly Lee Holcomb and Tyler Brocklehurst for their assistance.

Supplementary materials

Supplementary material associated with this article can be found, in the online version, at doi:10.1016/j.neuroimage.2021.117837.

References

Aron, A.R., Behrens, T.E., Smith, S., Frank, M.J., Poldrack, R.A., 2007. Triangulating a cognitive control network using diffusion-weighted magnetic resonance imaging (MRI) and functional MRI. J. Neurosci. 27, 3743–3752.
Aron, A.R., Robbins, T.W., Poldrack, R.A., 2014a. Inhibition and the right inferior frontal cortex: one decade on. Trends Cogn. Sci. 18, 177–185.
Aron, A.R., Robbins, T.W., Poldrack, R.A., 2014b. Right inferior frontal cortex: addressing the rebuttals. Front. Hum. Neurosci. 8, 905.
Beaton, L.E., Azma, S., Marinkovic, K., 2018. When the brain changes its mind: Oscillatory dynamics of conflict processing and response switching in a flanker task during alcohol challenge. PLoS One 13, e0191200.
Boehler, C.N., Appelbaum, L.G., Krebs, R.M., Chen, L.C., Woldorff, M.G., 2011. The role of stimulus salience and attentional capture across the neural hierarchy in a stop-signal task. PLoS One 6, e26386.
Braver, T.S., Barch, D.M., Gray, J.R., Molfese, D.L., Snyder, A., 2001. Anterior cingulate cortex and response conflict: effects of frequency, inhibition and errors. Cereb. Cortex 11, 825–836.
Breakspear, M., 2017. Dynamic models of large-scale brain activity. Nat. Neurosci. 20, 340–352.
Buxton, R.B., 2002. Introduction to Functional Magnetic Resonance Imaging. Cambridge University Press, New York, NY.
Chikazoe, J., Jimura, K., Asari, T., Yamashita, K.-i., Morimoto, H., Hirose, S., Miyashita, Y., Konishi, S., 2008. Functional dissociation in right inferior frontal cortex during performance of Go/No-Go task. Cereb. Cortex 19, 146–152.
Corbetta, M., Shulman, G.L., 2002. Control of goal-directed and stimulus-driven attention in the brain. Nat. Rev. Neurosci. 3, 201–215.
Correas, A., Lopez-Caneda, E., Beaton, L., Rodriguez Holguin, S., Garcia-Moreno, L.M., Anton-Toro, L.F., Cadaveira, F., Maestu, F., Marinkovic, K., 2019. Decreased event-related theta power and phase-synchrony in young binge drinkers during target detection: an anatomically-constrained MEG approach. J. Psychopharmacol. 33, 335–346.
Dale, A.M., Fischl, B., Sereno, M.I., 1999. Cortical surface-based analysis. I. Segmentation and surface reconstruction. Neuroimage 9, 179–194.
Dale, A.M., Liu, A.K., Fischl, B.R., Buckner, R.L., Belliveau, J.W., Lewine, J.D., Halgren, E., 2000. Dynamic statistical parametric mapping: combining fMRI and MEG for high-resolution imaging of cortical activity. Neuron 26, 55–67.

Dale, A.M., Sereno, M.I., 1993. Improved localization of cortical activity by combining EEG and MEG with MRI cortical surface reconstruction: a linear approach. J. Cogn. Neurosci. 5, 162–176.
Delorme, A., Makeig, S., 2004. EEGLAB: an open source toolbox for analysis of single-trial EEG dynamics including independent component analysis. J. Neurosci. Methods 134, 9–21.
Downar, J., Crawley, A.P., Mikulis, D.J., Davis, K.D., 2002. A cortical network sensitive to stimulus salience in a neutral behavioral context across multiple sensory modalities. J. Neurophysiol. 87, 615–620.
Duann, J.R., Ide, J.S., Luo, X., Li, C.S., 2009. Functional connectivity delineates distinct roles of the inferior frontal cortex and presupplementary motor area in stop signal inhibition. J. Neurosci. 29, 10171–10179.
Fischl, B., Sereno, M.I., Tootell, R.B., Dale, A.M., 1999. High-resolution intersubject averaging and a coordinate system for the cortical surface. Hum. Brain Mapp. 8, 272–284.
Frank, M.J., 2006. Hold your horses: a dynamic computational role for the subthalamic nucleus in decision making. Neural Netw. 19, 1120–1136.
Fries, P., 2005. A mechanism for cognitive dynamics: neuronal communication through neuronal coherence. Trends Cogn. Sci. 9, 474–480.
Garavan, H., Ross, T.J., Murphy, K., Roche, R.A., Stein, E.A., 2002. Dissociable executive functions in the dynamic control of behavior: inhibition, error detection, and correction. Neuroimage 17, 1820–1829.
Gramfort, A., Luessi, M., Larson, E., Engemann, D.A., Strohmeier, D., Brodbeck, C., Parkkonen, L., Hamalainen, M.S., 2014. MNE software for processing MEG and EEG data. Neuroimage 86, 446–460.
Halgren, E., Baudena, P., Clarke, J.M., Heit, G., Marinkovic, K., Devaux, B., Vignal, J.P., Biraben, A., 1995. Intracerebral potentials to rare target and distractor auditory and visual stimuli. II. Medial, lateral and posterior temporal lobe. Electroencephalogr. Clin. Neurophysiol. 94, 229–250.
Halgren, E., Marinkovic, K., 1995. Neurophysiological networks integrating human emotions. In: Gazzaniga, M. (Ed.), The Cognitive Neurosciences. MIT Press, Cambridge, MA, pp. 1137–1151.
Halgren, E., Sherfey, J., Irimia, A., Dale, A.M., Marinkovic, K., 2011. Sequential temporo-fronto-temporal activation during monitoring of the auditory environment for temporal patterns. Hum. Brain Mapp. 32, 1260–1276.
Hamalainen, M.S., Ilmoniemi, R.J., 1994. Interpreting magnetic fields of the brain: minimum norm estimates. Med. Biol. Eng. Comput. 32, 35–42.
Hampshire, A., 2015. Putting the brakes on inhibitory models of frontal lobe function. Neuroimage 113, 340–355.
Haynes, W.I., Haber, S.N., 2013. The organization of prefrontal-subthalamic inputs in primates provides an anatomical substrate for both functional specificity and integration: implications for Basal Ganglia models and deep brain stimulation. J. Neurosci. 33, 4804–4814.
Hein, G., Knight, R.T., 2008. Superior temporal sulcus–It's my area: or is it? J. Cogn. Neurosci. 20, 2125–2136.
Heston, J., Friedman, A., Baqai, M., Bavafa, N., Aron, A.R., Hnasko, T.S., 2020. Activation of subthalamic nucleus stop circuit disrupts cognitive performance. Eneuro 7.
Horstmann, G., 2006. Latency and duration of the action interruption in surprise. Cogn. Emot. 20, 242–273.
Ishihara, S., 1987. Test For Colour-Blindness. Kanehara Tokyo, Japan.
Knezevic, M., Marinkovic, K., 2017. Neurodynamic correlates of response inhibition from emerging to mid adulthood. Cogn. Dev. 43, 106–118.
Kovacevic, S., Azma, S., Irimia, A., Sherfey, J., Halgren, E., Marinkovic, K., 2012. Theta oscillations are sensitive to both early and late conflict processing stages: effects of alcohol intoxication. PLoS One 7, e43957.
Lachaux, J.P., Rodriguez, E., Martinerie, J., Varela, F.J., 1999. Measuring phase synchrony in brain signals. Hum. Brain Mapp. 8, 194–208.
Langner, R., Kellermann, T., Eickhoff, S.B., Boers, F., Chatterjee, A., Willmes, K., Sturm, W., 2012. Staying responsive to the world: modality-specific and-nonspecific contributions to speeded auditory, tactile, and visual stimulus detection. Hum. Brain Mapp. 33, 398–418.
Levy, B.J., Wagner, A.D., 2011. Cognitive control and right ventrolateral prefrontal cortex: reflexive reorienting, motor inhibition, and action updating. Ann. N. Y. Acad. Sci. 1224, 40–62.
Lin, F.H., Witzel, T., Hamalainen, M.S., Dale, A.M., Belliveau, J.W., Stufflebeam, S.M., 2004. Spectral spatiotemporal imaging of cortical oscillations and interactions in the human brain. Neuroimage 23, 582–595.
Lin, M.Y., Tseng, Y.J., Cheng, C.H., 2018. Age effects on spatiotemporal dynamics of response inhibition: an MEG Study. Front. Aging Neurosci. 10, 386.
Liu, A.K., Dale, A.M., Belliveau, J.W., 2002. Monte Carlo simulation studies of EEG and MEG localization accuracy. Hum. Brain Mapp. 16, 47–62.
Manza, P., Hu, S., Chao, H.H., Zhang, S., Leung, H.C., Li, C.R., 2016. A dual but asymmetric role of the dorsal anterior cingulate cortex in response inhibition and switching from a non-salient to salient action. Neuroimage 134, 466–474.
Marinkovic, K., 2004. Spatiotemporal dynamics of word processing in the human cortex. Neuroscientist 10, 142–152.
Marinkovic, K., Beaton, L.E., Rosen, B.Q., Happer, J.P., Wagner, L.C., 2019. Disruption of frontal lobe neural synchrony during cognitive control by alcohol intoxication. J. Vis. Exp. 144.
Marinkovic, K., Halgren, E., Maltzman, I., 2001. Arousal-related P3a to novel auditory stimuli is abolished by a moderately low alcohol dose. Alcohol Alcohol. 36, 529–539.
Marinkovic, K., Rosen, B.Q., Cox, B., Hagler Jr., D.J., 2014. Spatio-temporal processing of words and nonwords: hemispheric laterality and acute alcohol intoxication. Brain Res. 1558, 18–32.
Martin, A.B., Yang, X., Saalmann, Y.B., Wang, L., Shestyuk, A., Lin, J.J., Parvizi, J., Knight, R.T., Kastner, S., 2019. Temporal dynamics and response modulation across the human visual system in a spatial attention task: an ECoG study. J. Neurosci. 39, 333–352.
Medalla, M., Barbas, H., 2009. Synapses with inhibitory neurons differentiate anterior cingulate from dorsolateral prefrontal pathways associated with cognitive control. Neuron 61, 609–620.
Menon, V., Uddin, L.Q., 2010. Saliency, switching, attention and control: a network model of insula function. Brain Struct. Funct. 214, 655–667.
Morecraft, R.J., Geula, C., Mesulam, M.M., 1993. Architecture of connectivity within a cingulo-fronto-parietal neurocognitive network for directed attention. Arch. Neurol. 50, 279–284.
Nachev, P., Kennard, C., Husain, M., 2008. Functional role of the supplementary and pre-supplementary motor areas. Nat. Rev. Neurosci. 9, 856–869.
Nambu, A., 2004. A new dynamic model of the cortico-basal ganglia loop. Prog. Brain Res. 143, 461–466.
Oostenveld, R., Fries, P., Maris, E., Schoffelen, J.M., 2011. FieldTrip: open source software for advanced analysis of MEG, EEG, and invasive electrophysiological data. Comput. Intell. Neurosci. 2011, 156869.
Rae, C.L., Hughes, L.E., Anderson, M.C., Rowe, J.B., 2015. The prefrontal cortex achieves inhibitory control by facilitating subcortical motor pathway connectivity. J. Neurosci. 35, 786–794.
Ridderinkhof, K.R., van den Wildenberg, W.P., Segalowitz, S.J., Carter, C.S., 2004. Neurocognitive mechanisms of cognitive control: the role of prefrontal cortex in action selection, response inhibition, performance monitoring, and reward-based learning. Brain Cogn. 56, 129–140.
Rosen, B.Q., Padovan, N., Marinkovic, K., 2016. Alcohol hits you when it is hard: intoxication, task difficulty, and theta brain oscillations. Alcohol Clin. Exp. Res. 40, 743–752.
Sebastian, A., Jung, P., Neuhoff, J., Wibral, M., Fox, P.T., Lieb, K., Fries, P., Eickhoff, S.B., Tuscher, O., Mobascher, A., 2016. Dissociable attentional and inhibitory networks of dorsal and ventral areas of the right inferior frontal cortex: a combined task-specific and coordinate-based meta-analytic fMRI study. Brain Struct. Funct. 221, 1635–1651.
Serences, J.T., Shomstein, S., Leber, A.B., Golay, X., Egeth, H.E., Yantis, S., 2005. Coordination of voluntary and stimulus-driven attentional control in human cortex. Psychol. Sci. 16, 114–122.
Sharp, D.J., Bonnelle, V., De Boissezon, X., Beckmann, C.F., James, S.G., Patel, M.C., Mehta, M.A., 2010. Distinct frontal systems for response inhibition, attentional capture, and error processing. Proc. Natl. Acad. Sci. U. S. A. 107, 6106–6111.
Sokolov, E.N., 1963. Perception and the Conditioned Reflex. Pergamon Press, New York.
Sridharan, D., Levitin, D.J., Menon, V., 2008. A critical role for the right fronto-insular cortex in switching between central-executive and default-mode networks. Proc. Natl. Acad. Sci. 105, 12569–12574.
Stinear, C.M., Coxon, J.P., Byblow, W.D., 2009. Primary motor cortex and movement prevention: where Stop meets Go. Neurosci. Biobehav. Rev. 33, 662–673.
Swann, N., Tandon, N., Canolty, R., Ellmore, T.M., McEvoy, L.K., Dreyer, S., DiSano, M., Aron, A.R., 2009. Intracranial EEG reveals a time- and frequency-specific role for the right inferior frontal gyrus and primary motor cortex in stopping initiated responses. J. Neurosci. 29, 12675–12685.
Swann, N.C., Cai, W., Conner, C.R., Pieters, T.A., Claffey, M.P., George, J.S., Aron, A.R., Tandon, N., 2012. Roles for the pre-supplementary motor area and the right inferior frontal gyrus in stopping action: electrophysiological responses and functional and structural connectivity. Neuroimage 59, 2860–2870.
Swick, D., Ashley, V., Turken, U., 2011. Are the neural correlates of stopping and not going identical? Quantitative meta-analysis of two response inhibition tasks. Neuroimage 56, 1655–1665.
Swick, D., Chatham, C.H., 2014. Ten years of inhibition revisited. Front. Hum. Neurosci. 8, 329.
Uddin, L.Q., 2015. Salience processing and insular cortical function and dysfunction. Nat. Rev. Neurosci. 16, 55–61.
von Stein, A., Sarnthein, J., 2000. Different frequencies for different scales of cortical integration: from local gamma to long range alpha/theta synchronization. Int. J. Psychophysiol. 38, 301–313.
Wessel, J.R., 2018. An adaptive orienting theory of error processing. Psychophysiology 55, e13041.
Wessel, J.R., Aron, A.R., 2013. Unexpected events induce motor slowing via a brain mechanism for action-stopping with global suppressive effects. J. Neurosci. 33, 18481–18491.
Wessel, J.R., Aron, A.R., 2017. On the globality of motor suppression: unexpected events and their influence on behavior and cognition. Neuron 93, 259–280.